A R C H I V E S O F M E T A L L U R G Y A N D M A T E R I A L S
Volume 60 2015 Issue 1
DOI: 10.1515/amm-2015-0015

E. RUDNIK*, P. BISKUP**

ELECTROCHEMICAL STUDIES OF LEAD TELLURIDE BEHAVIOR IN ACIDIC NITRATE SOLUTIONS

ELEKTROCHEMICZNE BADANIA TELLURKU OŁOWIU W KWAŚNYCH ROZTWORACH AZOTANOWYCH

Electrochemistry of lead telluride stationary electrode was studied in nitric acid solutions of pH 1.5-3.0. E-pH diagram for Pb-Te-H_2O system was calculated. Results of cyclic voltammetry of Pb, Te and PbTe were discussed in correlation with thermodynamic predictions. Anodic dissolution of PbTe electrode at potential approx. -100÷50 mV (SCE) resulted in tellurium formation, while above 300 mV TeO_2 was mainly produced. The latter could dissolve to $HTeO_2^+$ under acidic electrolyte, but it was inhibited by increased pH of the bath.

Keywords: lead telluride; cyclic voltammetry; pH; nitric acid

Przeprowadzono elektrochemiczne badania zachowania się tellurku ołowiu w roztworach kwasu azotowego(V) o pH 1,5-3,0. Obliczono diagram równowagi E-pH dla układu Pb-Te-H_2O. Przedyskutowano wyniki pomiarów woltamperometrii cyklicznej Pb, Te i PbTe w odniesieniu do przewidywań termodynamicznych. Produktem utleniania tellurku ołowiu przy potencjałach ok. -100÷50 mV (NEK) jest tellur, natomiast powyżej 300 mV tworzy się przede wszystkim TeO_2, który ulega wtórnemu rozpuszczaniu w roztworze kwaśnym z utworzeniem $HTeO_2^+$. Proces jest hamowany przez wzrost pH elektrolitu.

1. Introduction

In recent years thin films of lead telluride have received a much attention due to its interesting physical properties. PbTe is a semiconductor with a narrow band gap (0.3 eV at 300 K) and good thermoelectric properties used mainly as infrared detectors and thermoelectric material [1]. Various methods are used for PbTe films preparation, but among them vacuum deposition techniques (e.g. thermal evaporation [2], molecular beam epitaxy [3]) has been used most often. Electrochemical deposition of PbTe has been developed since late 1990s [4, 5]. Most of the studies have been focused on the electrodeposition of lead telluride from acidic nitrate solutions [6-8], but alkaline bath with EDTA as Pb^{2+} complexing agent was also proposed [9, 10]. In contrary to other technologically and/or economically important tellurides, such as CdTe [11], Ag_2Te [12] or $AuTe_2$ [13, 14], very little is known on the fundamental electrochemistry of PbTe in aqueous solutions. To date the only exception is the paper of Strehblow and Bettini [15], who investigated the electrochemical reactions on PbTe in $HClO_4$, HNO_3 and HBr acids (pH 1.1), KOH (pH 12.9) or acetate buffer (pH 4.9). There have been not more detailed studies on the behavior of the bulk material at solution pH used usually during electrodeposition. Hence, the aim of this work was to give further insights into the electrochemical processes of lead telluride in acidic nitrate solutions. Cyclic voltammetry in solutions with pH in the range of 1.5-3.0 is discussed. The results are compared with a behavior of pure lead and tellurium as well as with thermodynamic predictions.

2. Experimental

Electrochemical behavior of lead telluride (99.998% Aldrich) was studied in HNO_3 solutions in the pH range of 1.5-3.0. Lead (99.999% Alfa) and tellurium (99.9%) was also investigated for comparison. All electrodes were prepared from metallic pieces embedded in duracryl resin leaving one active surface. Surface active area of each electrode was 1-2 cm^2. Prior to each experiment tellurium samples were polished with diamond slurry (with the grain gradation of 3 μm and 1 μm). The electrodes were then thoroughly rinsed in deionized water and acetone (each stage was carried out in a laboratory ultrasonic cleaner for 10 min). The stationary tellurium electrodes in non agitated baths (100 cm^3) were used. Each measurement was carried out with fresh electrode surface and fresh portion of the electrolyte. Platinum plate (6 cm^2) was used as the counter electrode. The reference electrode was saturated calomel electrode (SCE) and all potentials are reported against this electrode. Electrochemical measurements (principally cyclic voltammetry) were made using a potentiostat (Atlas Sollich 98 EII). Potentials of the working electrode were ranging from -1800 mV to 1300 mV (SCE) to cover all reac-

* AGH UNIVERSITY OF SCIENCE AND TECHNOLOGY, FACULTY OF NON-FERROUS METALS, DEPARTMENT OF PHYSICAL CHEMISTRY AND METALLURGY OF NON-FERROUS METALS, AL. A. MICKIEWICZA 30, 30-059 KRAKÓW, POLAND
** ROYAL GROUP, PO BOX 5151, EASTERN RING ROAD, ABU DHABI, UNITED ARAB EMIRATES

tions of interest in the investigated system. The potential range was scanned in both positive-going and negative-going sweeps with various scan rates (1-100 mV/s). For detailed analysis, CV scans were registered in narrower potential ranges at a scan rate of 10 mV/s. Potentiostatic anodic dissolution of lead telluride was also carried out. Before and after potentiostatic measurement the electrode surface was observed by means of optical and scanning electron microscopes. Solid products of lead telluride anodic oxidation were analyzed with SEM-EDS (Hitachi S 4700), whereas concentration of tellurium species soluble in the electrolyte was determined by means of ICP method (Perkin Elmer ICP AES "Plasma 40"). All experiments were performed at room temperature and repeated a few times to check the reproducibility of the results.

3. Results and discussion

3.1. E-pH diagram of PbTe-H_2O system

The E-pH diagram of PbTe-H_2O system was calculated on the basis of the thermodynamic data summarized in Table 1. The anhydrous forms of TeO_2 and red PbO were considered, since they are more stable than the hydrated form $TeO_2 \cdot H_2O$ and yellow PbO, respectively. Table 2 shows all chemical and electrochemical reactions considered for this system in the pH range from -1 to 10 at temperature of 298 K. The Nernst equations showing the relationships between concentrations of soluble species, solution pH and equilibrium potentials are reported. pH dependences on ions concentration for chemical equilibriums are also presented.

TABLE 1

Thermodynamic data used for calculation of E-pH diagram of PbTe-H_2O system (298 K, 10^5 Pa) [16, 17]

Compound	ΔG^o [J· mol^{-1}]
Te^{4+}	219 472
Te^{2-}	220 813
Te_2^{2-}	162 363
HTe^-	157 963
H_2Te_{aq}	142 879
$HTeO_2^+$	-261 917
TeO_2 (anhydrous)	-273 691
TeO_3(anhydrous)	-314 116
$HTeO_3^-$	-437 185
TeO_3^{2-}	-392 980
H_2TeO_4	-551 647
$HTeO_4^-$	-516 493
TeO_4^{2-}	-457 079
Pb^{2+}	-24 318
Pb^{4+}	302 937
PbO (anhydrous, red)	-189 598
PbO_2	-219 305
Pb_3O_4	-618 444
PbH_2	291 205
PbTe	-63 928
H_2O_l	-237 531

TABLE 2

Thermodynamic expressions for the PbTe-H_2O system (298 K, 10^5 Pa)

No.	Reactions	Equilibrium potentials vs NHE [V] or pH expression
a	$H_2 \rightarrow 2H^+ + 2e$	$E_o = -0.059pH$
b	$2H_2O \rightarrow O_2 + 4H^+ + 4e$	$E_o = 1.228 - 0.059pH$
1	$Pb + Te^{2-} \rightarrow PbTe + 2e$	$E_o = -1.475 - 0.0295\log[Te^{2-}]$
2	$Pb + {}^1/_2\ Te_2^{2-} \rightarrow PbTe + e$	$E_o = -1.504 - 0.0295\log[Te_2^{2-}]$
3	$Pb + HTe^- \rightarrow PbTe + 2H^+ + 2e$	$E_o = -1.150 - 0.059pH - 0.0295\log[HTe^-]$
4	$Pb + H_2Te \rightarrow PbTe + 2H^+ + 2e$	$E_o = -1.072 - 0.059pH - 0.0295\log[H_2Te]$
5	$PbTe \rightarrow Pb^{2+} + Te + 2e$	$E_o = 0.205 + 0.0295\log[Pb^{2+}]$
6	$PbTe \rightarrow Pb^{2+} + Te^{4+} + 6e$	$E_o = 0.447 + 0.01\log([Pb^{2+}][Te^{4+}])$
7	$PbTe + 2H_2O \rightarrow Pb^{2+} + HTeO_2^+ + 3H^+ + 6e$	$E_o = 0.437 - 0.0295pH + 0.01\log([Pb^{2+}][HTeO_2^+])$
8	$PbTe + 2H_2O \rightarrow Pb^{2+} + TeO_2 + 4H^+ + 6e$	$E_o = 0.416 - 0.039pH + 0.01\log[Pb^{2+}]$
9	$PbTe + 3H_2O \rightarrow Pb^{2+} + HTeO_3^- + 5H^+ + 6e$	$E_o = 0.544 - 0.049pH + 0.0098\log([Pb^{2+}][HTeO_3^-])$
10	$PbTe + 3H_2O \rightarrow Pb^{2+} + TeO_3 + 6H^+ + 8e$	$E_o = 0.567 - 0.044pH + 0.007\log[Pb^{2+}]$
11	$PbTe + H_2O \rightarrow PbO + Te + 2H^+ + 2e$	$E_o = 0.580 - 0.059pH$
12	$PbTe + H_2O \rightarrow PbO + Te^{4+} + 2H^+ + 6e$	$E_o = 0.572 - 0.02pH + 0.0098\log[Te^{4+}]$
13	$PbTe + 3H_2O \rightarrow PbO + HTeO_2^+ + 5H^+ + 6e$	$E_o = 0.561 - 0.049pH + 0.01\log[HTeO_2^+]$
14	$PbTe + 3H_2O \rightarrow PbO + TeO_2 + 6H^+ + 6e$	$E_o = 0.541 - 0.059pH$
15	$PbTe + 4H_2O \rightarrow PbO + HTeO_3^- + 7H^+ + 6e$	$E_o = 0.669 - 0.069pH + 0,0098\log[HTeO_3^-]$
16	$PbTe + 4H_2O \rightarrow PbO + TeO_3^{2-} + 8H^+ + 6e$	$E_o = 0.745 - 0.079pH + 0,0098\log[TeO_3^{2-}]$
17	$PbTe + 4H_2O \rightarrow PbO + TeO_3 + 8H^+ + 8e$	$E_o = 0.661 - 0.059pH$
18	$PbTe + 2H_2O \rightarrow PbO_2 + Te^{2-} + 4H^+ + 2e$	$E_o = 2.801 - 0.118pH + 0.0295\log[Te^{2-}]$
19	$PbTe + 2H_2O \rightarrow PbO_2 + HTe^- + 3H^+ + 2e$	$E_o = 2.475 - 0.089pH + 0.0295\log[HTe^-]$
20	$PbTe + 2H_2O \rightarrow PbO_2 + H_2Te + 2H^+ + 2e$	$E_o = 2.397 - 0.059pH + 0.0295\log[H_2Te]$
21	$PbH_2 + Te \rightarrow PbTe + 2H^+ + 2e$	$E_o = -1.840 - 0.059pH - 0.0295\log p_{PbH_2}$

cd. TABLE 2

22	$H_2Te \rightarrow Te + 2H^+ + 2e$	$E_o = -0.740 - 0.059pH - 0.0295\log[H_2Te]$
23	$2H_2Te \rightarrow Te_2^{2-} + 4H^+ + 2e$	$E_o = -0.639 - 0.118pH + 0.0295\log\frac{[Te_2^{2-}]}{[H_2Te]^2}$
24	$2HTe^- \rightarrow Te_2^{2-} + 2H^+ + 2e$	$E_o = -0.796 - 0.059pH + 0.0295\log\frac{[Te_2^{2-}]}{[HTe^-]^2}$
25	$H_2Te \rightarrow HTe^- + H^+$	$pH = 2.645 + \log\frac{[HTe^-]}{[H_2Te]}$
26	$HTe^- \rightarrow Te^{2-} + H^+$	$pH = 11.02 + \log\frac{[Te^{2-}]}{[HTe^-]}$
27	$2Te^{2-} \rightarrow Te_2^{2-} + 2e$	$E_o = -1.447 + 0.0295\log\frac{[Te_2^{2-}]}{[Te^{2-}]^2}$
28	$Te \rightarrow Te^{4+} + 4e$	$E_o = 0.569 + 0.015\log[Te^{4+}]$
29	$Te + 2H_2O \rightarrow TeO_2 + 4H^+ + 4e$	$E_o = 0.522 - 0.059pH$
30	$Te + 2H_2O \rightarrow HTeO_2^+ + 3H^+ + 4e$	$E_o = 0.552 - 0.044pH + 0.015\log[HTeO_2^+]$
31	$Te^{4+} + 4H_2O \rightarrow H_2TeO_4 + 6H^+ + 2e$	$E_o = 0.927 - 0.177pH + 0.0295\log\frac{[H_2TeO_4]}{[Te^{4+}]}$
32	$Te^{4+} + 2H_2O \rightarrow HTeO_2^+ + 3\,H^+$	$pH = -0.37 + 0.33\log\frac{[HTeO_2^+]}{[Te^{4+}]}$
33	$Te^{4+} + 3H_2O \rightarrow TeO_3 + 6H^+ + 2e$	$E_o = 0.927 - 0.177pH - 0.0295\log[Te^{4+}]$
34	$HTeO_2^+ + H_2O \rightarrow TeO_3 + 3H^+ + 2e$	$E_o = 0.960 - 0.088pH - 0.0295\log[HTeO_2^+]$
35	$HTeO_2^+ \rightarrow TeO_2 + H^+$	$pH = -2.06 - \log[HTeO_2^+]$
36	$HTeO_2^+ + 2H_2O \rightarrow HTeO_4^- + 4H^+ + 2e$	$E_o = 1.14 - 0.118pH + 0.0295\log\frac{[HTeO_4^-]}{[HTeO_2^+]}$
37	$TeO_2 + H_2O \rightarrow TeO_3 + 2H^+ + 2e$	$E_o = 1.02 - 0.059pH$
38	$TeO_2 + H_2O \rightarrow HTeO_3^- + H^+$	$pH = 12.98 + \log[HTeO_3^-]$
39	$TeO_2 + 2H_2O \rightarrow HTeO_4^- + 3H^+ + 2e$	$E_o = 1.20 - 0.089pH + 0.0295\log[HTeO_4^-]$
40	$HTeO_4^- \rightarrow TeO_4^{2-} + H^+$	$pH = 10.42 + \log\frac{[TeO_4^{2-}]}{[HTeO_4^-]}$
41	$TeO_3 + H_2O \rightarrow HTeO_4^- + H^+$	$pH = 6.16 + \log[HTeO_4^-]$
42	$HTeO_3^- \rightarrow TeO_3^{2-} + H^+$	$pH = 7.75 + \log\frac{[TeO_3^{2-}]}{[HTeO_3^-]}$
43	$HTeO_3^- + H_2O \rightarrow HTeO_4^- + 2H^+ + 2e$	$E_o = 0.820 - 0.059pH + 0.0295\log\frac{[HTeO_4^-]}{[HTeO_3^-]}$
44	$Pb \rightarrow Pb^{2+} + 2e$	$E_o = -0.126 + 0.0295\log[Pb^{2+}]$
45	$Pb + H_2O \rightarrow PbO + 2H^+ + 2e$	$E_o = 0.248 - 0.059pH$
46	$3PbO + H_2O \rightarrow Pb_3O_4 + 2H^+ + 2e$	$E_o = 0.973 - 0.059pH$
47	$Pb_3O_4 + 2H_2O \rightarrow 3PbO_2 + 4H^+ + 4e$	$E_o = 1.128 - 0.059pH$
48	$Pb^{2+} \rightarrow Pb^{4+} + 2e$	$E_o = 1.696 + 0.0295\log\frac{[Pb^{4+}]}{[Pb^{2+}]}$
49	$3Pb^{2+} + 4H_2O \rightarrow Pb_3O_4 + 8H^+ + 2e$	$E_o = 2.097 - 0.239pH - 0.088\log[Pb^{2+}]$
50	$Pb^{2+} + 2H_2O \rightarrow PbO_2 + 4H^+ + 2e$	$E_o = 1.451 - 0.118pH - 0.0295\log[Pb^{2+}]$
51	$Pb^{2+} + H_2O \rightarrow PbO + 2H^+$	$pH = 6.33 - 0.5\log[Pb^{2+}]$
52	$Pb^{4+} + 2H_2O \rightarrow PbO_2 + 4H^+$	$pH = -2.07 - 0.25\log[Pb^{4+}]$
53	$PbH_2 \rightarrow Pb + 2H^+ + 2e$	$E_o = -1.509 - 0.059pH - 0.0295\log p_{PbH_2}$

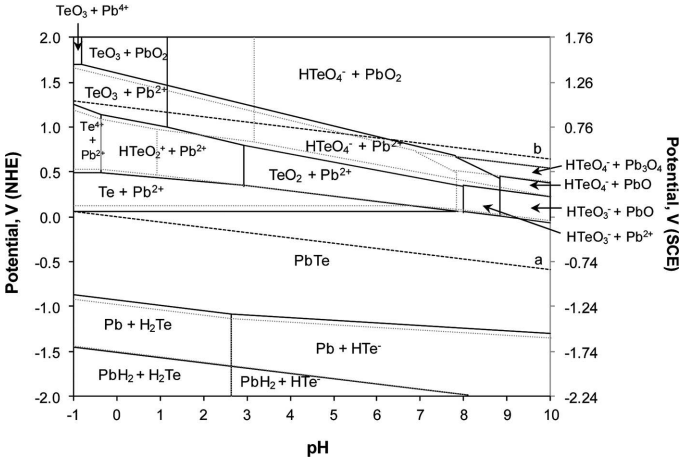

Fig. 1. E-pH diagram for Pb-Te-H_2O system at ions concentrations of 10^{-5} M (black lines) and 10^{-3} M (dotted gray lines)

Fig. 1 shows the domains of relative predominance of insoluble compounds and ionic forms for two concentrations of dissolved tellurium and lead species (10^{-5} M and 10^{-3} M). This diagram is valid only in the absence of substances with which tellurium or lead can form complexes or insoluble salts. Hence, it is appropriate for nitrate solutions.

From Fig. 1 appears that lead telluride PbTe is thermodynamically stable in aqueous solutions (free of oxidizing agents) in the whole studied pH range, since its stability domains lies above the line representing equilibrium of hydrogen electrode. Depending on the concentration, anodic oxidation at pHs below 7-8 converts Te^{2-} form in the solid PbTe into elemental tellurium or insoluble TeO_2, releasing Pb^{2+} ions. At higher pH PbTe surface can cover with a mixture of tellurium(IV) and lead(II) oxides. Direct transformation of PbTe into soluble tellurium species is thermodynamically declined. On the other hand, cathodic deposition of PbTe from the solutions containing $HTeO_2^+$ and Pb^{2+} is accompanied by deposition of thin layer of elemental tellurium followed by direct PbTe formation at potentials higher than equilibrium potential of Pb/Pb^{2+} electrode. Such phenomenon is energetically favorable during electrodeposition of metal tellurides from acidic solutions.

The electrolytic reduction of PbTe can produce elemental lead accompanied by evolution of hydrogen telluride H_2Te or telluride HTe^- formation below and above pH of 2.6, respectively.

Increase in the concentrations of the soluble species changes the pH regions of the stability of the individual compounds and formation of sparingly soluble oxides is expected in much more wide pH ranges.

3.2. Cyclic voltammetry of Pb and Te

Fig. 2 shows cyclic voltammograms for elemental lead and tellurium registered at pH 1.5-3.0. Results obtained for lead (Fig. 2a) are typical for simple metallic electrode and are consistent with the E-pH data for Pb-H_2O system [16]. An anodic part of the curve (A) represents dissolution of lead followed by the reduction of Pb^{2+} ions in the backward step (C1). Equilibrium potential for the Pb/Pb^{2+} electrode calculated according to the Nernst equation is in the range of -540 -510 mV (all values vs. SCE) for Pb^{2+} concentrations from 10^{-6} M to 10^{-5}M. The values are close to that obtained in the experiment. Cathodic parts (C2) of the voltammograms registered at potentials below -900 mV represent hydrogen evolution on the lead surface. Equilibrium potential of hydrogen electrode is dependent on the solution pH and it changes from -330 mV at pH 1.5 to -420 mV at pH 3.0. In fact, hydrogen evolution on lead occurs at much lower potentials due to high overpotential (-640 mV for current density of 50 $\mu A \cdot cm^{-2}$ [18]), hence the reaction is expected below -970 mV and it is dependent on the pH as it was found experimentally.

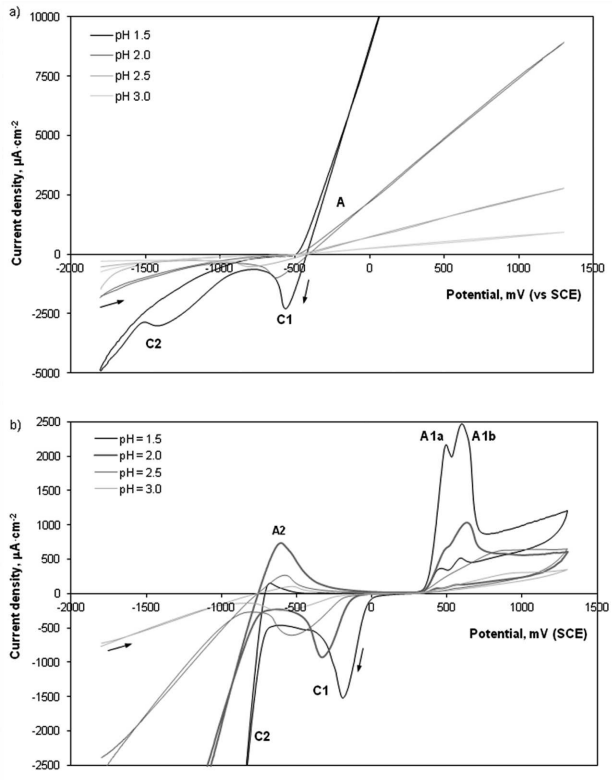

Fig. 2. Cyclic voltammograms of elements in HNO_3 solutions: a) lead, b) tellurium (10 mV/s)

Cyclic voltammograms for tellurium (Fig.2b) are much more complicated, since it can form compounds at various oxidation states [16]. Three anodic peaks in the positive-going initial scans and two cathodic responses in the backward step were found in the plots. The potential scan started at -1800 mV and it was accompanied by the flow of the cathodic current (C2), but above -740 ÷-710 mV the anodic peak (A2) appeared. At potentials from approx. -330 mV to approx. 300 mV a low anodic current density region was observed. The anodic current increased again above 330 ÷350 mV giving a double peak (A1). The last one degenerated gradually into one wide peak when pH of the electrolyte was increased from 1.5 to 3.0. In the backward sweep, the cathodic peak (C1) was observed in the potential range below 0 mV. Further decrease in the potential lead to the cathodic current flow (C2) with the negative-going curves overlapped previous positive-going sections of the voltammograms. As the solution pH was increased both anodic peaks A1a and A1b became lower in heights, turned gradually into one wide peak with a maximum slightly shifted towards more positive potentials. The cathodic peak C1 was also reduced, it grew wider and displaced to more negative potentials, simultaneously. The cathodic currents in the C2 region decreased seriously from approx. 30 $mA \cdot cm^{-2}$ at pH 1.5 to approx. 0.75 $mA \cdot cm^{-2}$ at pH 3.0 at the final potential of -1800 mV. The anodic peak A2 enlarged with the pH change from 1.5 to 2.0, but further increase in the pH was accompanied by the reduction and slight shifting of the peak maximum towards more positive potentials. The CV curves showed that increase in the solution pH inhibited gradually both anodic processes occurring at potentials above 330 mV and both cathodic reactions.

Detailed analysis of the results [19] showed that cathodic polarization of tellurium electrode below -800 mV (C2) was accompanied by evolution of hydrogen and H_2Te, but the latter was then oxidized at the potentials of approx. -700 mV (A2). H_2Te generated in the electrochemical reaction decomposed to elemental tellurium as black powdery precipitates in the bulk of the solution and a bright film drifting on the electrolyte surface. Two products could be formed at potentials above 300 mV: soluble $HTeO_2^+$ (500 mV, A1a) and sparingly soluble H_2TeO_3 i.e. hydrous TeO_2 (650 mV, A1b), but both seemed to be intermediate products for anhydrous TeO_2 precipitation on the electrode surface (detected with SEM/EDS on dry tellurium electrode [19]). Formation of the solid product as porous layer was almost undisturbed and no electrode passivation was observed.TeO_2 can dissolve to $HTeO_2^+$ under acidic electrolyte, but this process was hindered by pH increase (as it is suggested by the changes of the peak C1, representing reduction of $HTeO_2^+$ ions).

Equilibrium potentials calculated for Te/H_2TeO_3, $Te/HTeO_2^+$ and Te/TeO_2 show that with the increase in the electrode potential above 100 mV formation of soluble Te(IV) species from elemental tellurium followed by oxidation to solids is thermodynamically expected. The difference in the maximum potentials A1a and A1b at pH 1.5 was approx. 150 mV and it seems to be in accordance with the difference of the equilibrium potentials for Te/H_2TeO_3 (284 mV) and $Te/HTeO_2^+$ (170 mV) electrodes. At higher pH formation of tellurium oxide should be promoted due to its less solubility.

3.3. Cyclic voltammetry of PbTe

Fig. 3 shows cyclic voltammograms of PbTe in diluted nitric acid solutions. As it was observed previously for lead and tellurium, electrochemical behavior of the telluride is pH-dependent. The potential scan started at -1800 mV and it was accompanied by the flow of the cathodic current (C2), but above -170 mV small anodic peak (A2) appeared. Above potentials approx. 300 mV the increase in the anodic current density was observed (A1). In the reverse sweep, a wide cathodic peak (C1) was observed in the potential range below 0 mV, but its maximum was strongly dependent on the solution pH (maximum of the peak decreased and shifted towards more negative potentials with increased pH of the electrolyte). Further decrease in the potential (below -900 mV) lead to the cathodic current flow (C2) with the negative-going curves overlapped previous positive-going sections of the voltammograms.

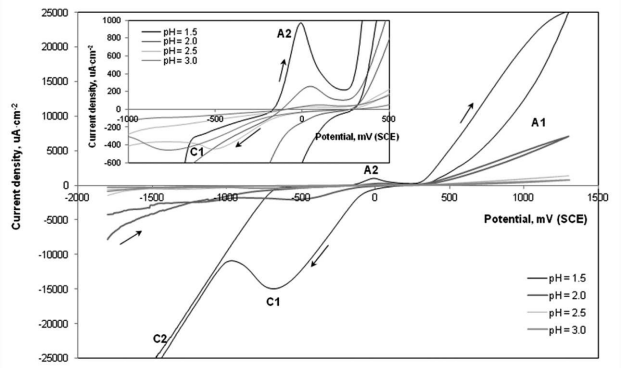

Fig. 3. Cyclic voltammograms for PbTe in HNO_3 solutions (10 mV/s)

Increase in the sweep rate (Fig. 4) changes the course of the CV curves in a typical way increasing the maxima of the peaks. However, for the cathodic peak at about -600 mV increased sweep rate resulted finally in the limiting current plateau (50-100 mV/s) indicating that soluble species are reduced at this potential range.

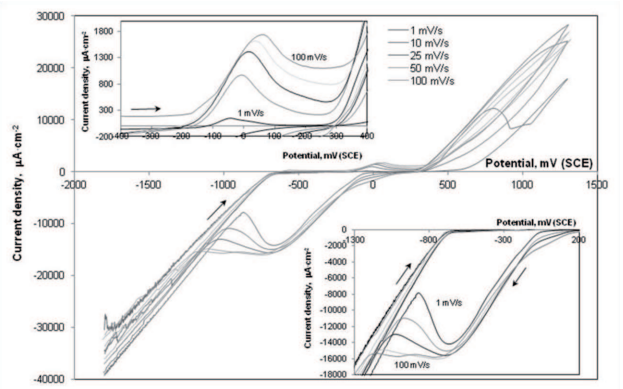

Fig. 4. The influence of the sweep rate on the course of the CV curves for PbTe in HNO_3 (pH 1.5)

The electrochemical behavior of PbTe electrode in narrower ranges of the potential was also studied. Fig.5 shows exemplary results. It was found that cathodic current corresponding to the C1 peak starts to flow only during the backward scan, demonstrating reduction of the species produced formerly at the potential range of the A1 peak. The C1 peak does not exist when potential scan was initiated below 300 mV.

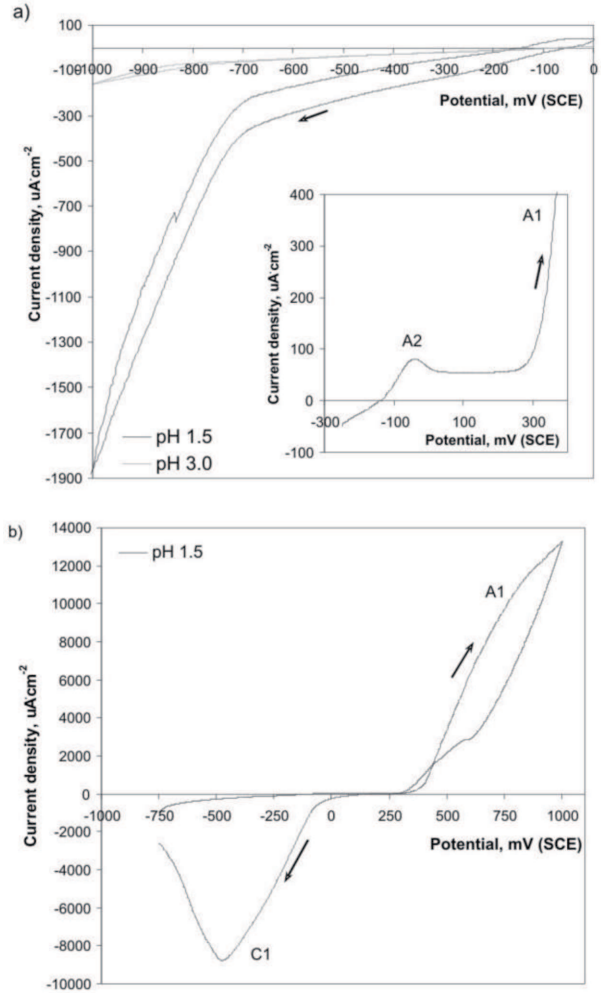

Fig. 5. CV curves for PbTe registered in narrow potential ranges: a) 0 ÷-1000 mV (inset: -300 ÷400 mV; pH 1.5), b) -750 ÷1000 mV

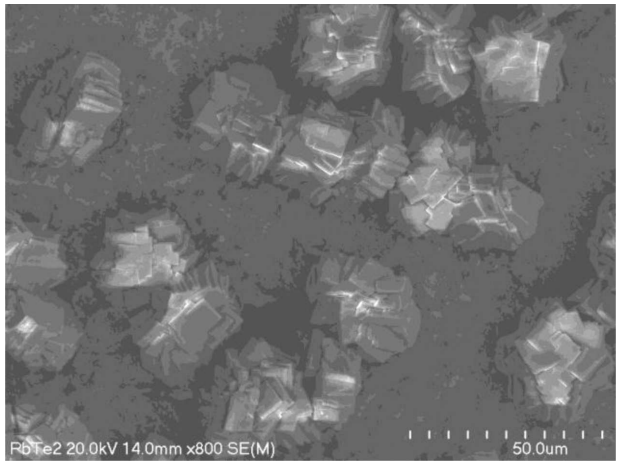

Fig. 6. Morphology of the PbTe surface anodically oxidized in HNO_3 of pH 1.5

PbTe electrode was oxidized at constant potentials of 0 and 800 mV for the same time (30 min). Fig. 6 shows the surface of the oxidized sample. SEM observations revealed the presence of characteristic crystals with the Te:O atomic ratio equaled 1:1.9 corresponding to TeO_2. Analysis of the

even areas of the electrode surface showed the presence of Pb, Te and O in the atomic ratio of 1:1.37:2.02.

Analysis of the solutions obtained after anodic oxidation of the PbTe electrode at pH of 1.5 at the potentials of 0 and 800 mV showed that concentration of tellurium species was comparable (0.5 mg/dm^3 and 0.4 mg/dm^3, respectively). It suggests that oxidation of the PbTe results in formation of soluble products, but they can form in the secondary processes of chemical dissolution of the sparingly soluble compounds.

3.4. Discussion

Comparison of the E-pH diagram and experimental results shows that anodic oxidation of the PbTe gives two primary products. At the potential of about -100 ÷50 mV formation of thin tellurium layer is expected:

$$PbTe \rightarrow Pb^{2+} + Te + 2e \quad (1)$$

This is accordant with the equilibrium potential -100 mV (SCE) calculated for 10^{-3}M concentration. Moreover, small anodic peaks observed in the CV curves confirm that the process run slowly.

Above 300 mV formation of TeO_2 is predicted by E-pH diagram:

$$PbTe + 2H_2O \rightarrow Pb^{2+} + TeO_2 + 4H^+ + 6e \quad (2)$$

However, detection of soluble tellurium species in the acidic solutions and formation of the C1 cathodic peak indicates competing growth and dissolution of TeO_2 product:

$$TeO_2 + H^+ \rightarrow HTeO_2^+ \quad (3)$$

The latter is in the agreement with tellurium behavior, since cathodic responses C1 can be correlated with reduction of tellurium(IV) species in acidic bath:

$$HTeO_2^+ + 3H^+ + 4e \rightarrow Te + 2H_2O \quad (4)$$

Obtained results are similar to the data reported by Strehblow and Bettini [15] who found that TeO_2 is a main product of the PbTe oxidation in acetate buffer (pH 4.9), but at higher potentials PbO was detected in the surface layer, probably as a result of the reaction:

$$PbTe + 2H_2O \rightarrow PbO + TeO_2 + 4H^+ + 6e \quad (5)$$

4. Conclusions

Electrochemistry of lead telluride was studied in acidic nitrate solutions with pH 1.5÷3.0. Predictions from E-pH diagrams were compared with experimental results of cyclic voltammograms of PbTe as well as Pb and Te in acidic solutions. Two products of the anodic PbTe dissolution are expected to form at potentials above -100 mV (SCE): thin Te layer and TeO_2. TeO_2 can dissolve to $HTeO_2^+$ under acidic electrolyte, but this process was hindered by pH increase.

Acknowledgements

This research study was financed from funds of Ministry of Science and Higher Education as a development project No. N R07 0017 04.

REFERENCES

[1] D.M. Rowe, CRC Handbook of thermoelectric, Boca Raton 1995.
[2] S. Kumar, Z.H. Khan, M.A. Majeed Khan, M. Husain, Current Applied. Phys. **5**, 561 (2005).
[3] H. Zogg, K. Alchalabi, D. Zimin, Demence Sci. J **51**, 53 (2001).
[4] F. Xiao, C. Hangarter, B. Yoo, Y. Rheem, K-H. Lee, N.V. Myung, Electrochim. Acta **53**, 8103-8117 (2008).
[5] M. Bouroushian, Electrochemistry of metal chalcogenides, Berlin Heidelberg 2010.
[6] L. Beaunier, H. Cachet, R. Cortes, M. Froment, J. Electroanal. Chem. **532**, 215 (2002).
[7] A. Mondal, N. Mukherjee, S.K. Bhar, D. Banerjee, Thin Solid Films **515**, 1255 (2006).
[8] Y.A. Ivanova, D.K. Ivanou, E.B. Streltsov, Electrochem. Comm. **9**, 599 (2007).
[9] H. Saloniemi, T. Kanniainen, M. Ritala, M. Leskelä, Thin Solid Films **326**, 78 (1998).
[10] H. Saloniemi, M. Kemmel, M. Ritala, M. Leskelä, J. Electroanal. Chem. **482**, 139 (2000).
[11] J. McHardy, F. Ludwig (Eds.), Electrochemistry of semiconductors and electronics, New Jersey 1992.
[12] M. Perdicakis, N. Grosselin, J. Bessiere, Electrochim. Acta **42** (20-22), 3351 (1997).
[13] S. Jayasekera, J. Avraamides, I.M. Ritchie, Electrochim. Acta **41**(6), 879 (1996).
[14] S.A. Salinas, M.A. Romero, I. Gonzalez, J. Appl. Electrochem. **28**, 417 (1998).
[15] H.H. Strehblow, M. Bettini, J. Electrochem. Soc. **127**(4), 847 (1980).
[16] M. Pourbaix, Atlas of electrochemical equilibria in aqueus solutions, New York 1966.
[17] K.C. Mills, Thermodynamic data for inorganic sulphides, selenides and tellurides, Butterworths 1974.
[18] C.K. Gupta, Chemical metallurgy: principles and practice, Weinheim 2003.
[19] E. Rudnik, J. Sobesto, Cyclic voltammetric studies of tellurium in diluted HNO_3 solutions, Arch. Metall. Mater. **56** (2), 271 (2011).

Received: 20 February 2014.